J|A|C|S COMMUNICATIONS

Published on Web 04/20/2009

NMR Analysis of the Architecture and Functional Remodeling of a Modular Multidomain Protein, RPA

Chris A. Brosey, Marie-Eve Chagot, Mark Ehrhardt,† Dalyir I. Pretto, Brian E. Weiner, and Walter J. Chazin*

Departments of Biochemistry and Chemistry, and Center for Structural Biology, Vanderbilt University, Nashville, Tennessee 37232-8725

Received February 21, 2009; E-mail: walter.chazin@vanderbilt.edu

The progression of DNA replication and repair requires the coordinated action of dynamic, multiprotein assemblies. We have previously proposed a critical role for proteins composed of multiple, flexibly attached domains in facilitating the action of these dynamic complexes.[1] Because these proteins can undergo intra- and interdomain rearrangements, they are able to interact optimally with the ever-changing substrate landscape present during DNA processing. RPA is a prototypical modular multidomain DNA processing protein with flexible linkers of various lengths (Figure 1). The trimer core is a compact assembly of three OB-fold domains

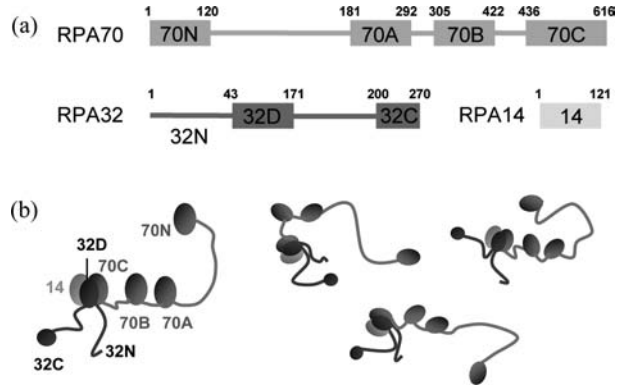

Figure 1. (a) Domain organization of RPA. All domains are OB-folds, except for RPA32C, which is a winged-helix domain, and the disordered functional domain RPA32N. (b) Illustration of "structural dynamics" and time-dependent RPA architecture.

(RPA70C/32D/14) to which is appended the disordered RPA32N functional domain, the RPA32C winged-helix domain, and the tandem RPA70AB and the RPA70N OB-fold domains. Despite a wealth of information available on the structure and function of these domains, very few insights have been obtained about the architecture of intact RPA.[2]

NMR spectroscopy in solution is a powerful tool for characterizing proteins under conditions that preserve intrinsic dynamic properties. The advent of TROSY, CRINEPT, and related experimental approaches[3] has vastly increased the upper limit of molecular masses accessible to study by NMR. Examples range from the globular malate synthase (82 kDa) to the oligomeric GroEL−GroES complex (872 kDa) to highly flexible domains from the ribosome (>2.5 MDa).[4] In the case of RPA (116 kDa) and many other multidomain proteins, modularity and interdomain flexibility are the critical properties that enable characterization of dynamic architectures by NMR.

To illustrate the analytical framework, results are presented first for RPA70NAB (M_r 45.8 kDa), which has an asymmetric arrangement with a 70-residue N−A linker and a 10-residue A−B linker (Figure 1). The $^{15}N-^{1}H$ TROSY-HSQC spectrum of ^{15}N-enriched RPA70NAB reveals the presence of over 370 of the 400 expected signals from 422 residues (Figure 2). The signals from each of the three domains appear in positions remarkably similar to those in NMR spectra of the three isolated domains (Figure S1). Thus, all three domains are structurally independent and resonance assignments can be transferred from the isolated domains to RPA70NAB.[5] NMR is highly sensitive to differences in the degree of interdomain flexibility; the signals from the A and B domains are substantially weaker than the signals from the N domain, even though all three domains are approximately the same mass (Figure 2). The differences arise from the fact that although the A and B domains are structurally independent, the short A−B tether partially restricts their motions, whereas the much longer N−A tether enables the N domain to tumble essentially freely in solution. The coupling of the A and B domains by the short tether is a critical factor for the ability to bind ssDNA with high affinity.[5]

The same approach was applied to the analysis of full-length RPA. Figure 2b shows the remarkably high quality $^{15}N-^{1}H$ TROSY-HSQC spectrum of $^{2}H,^{15}N$-enriched RPA. Over 350 of the 550 expected signals from the RPA70N, RPA70A, RPA70B, RP32C, and RPA32N domains were identified in this spectrum. As in the case of RPA70NAB, the signals appear in nearly identical positions as in the NMR spectra of the isolated domains, indicating the domains are structurally independent and enabling the transfer of resonance assignments directly to the intact protein (Figure 2c). Moreover, a clear hierarchy in the interdomain dynamics was evident. The signals from RPA32N and RPA32C were very strong, indicating that these domains are nearly as flexible in the trimer as when isolated on their own. Lower intensity is observed for the signals from RPA70 N, A, and B domains, with N signals stronger than A and B as seen for RPA70NAB. In contrast, no signals were identified for the RPA70C/RPA32D/RPA14 trimer core. Although it has a relatively large mass (M_r 49.1 kDa), the trimer core on its own gives excellent spectra (Figure S2). The absence of signals in the intact protein is therefore attributable to the slowing of its rate of tumbling due to the drag caused by the attachment of the five other domains. The ability to simultaneously probe five domains without interference from the trimer core in the TROSY-HSQC spectrum demonstrates the value of the dynamic hierarchy of different NMR experiments.

Having established a basis for analyzing RPA architecture, investigations were undertaken to characterize the remodeling of RPA structural dynamics upon binding ssDNA. Figure 2c shows a comparison of a region from $^{15}N-^{1}H$ TROSY-HSQC spectra of $^{2}H,^{15}N$-enriched RPA obtained in the absence and presence of dT_{30},

† Current address: Monsanto Company, 800 N. Lindbergh Blvd., St. Louis, MO 63167.

10.1021/ja9013634 CCC: $40.75

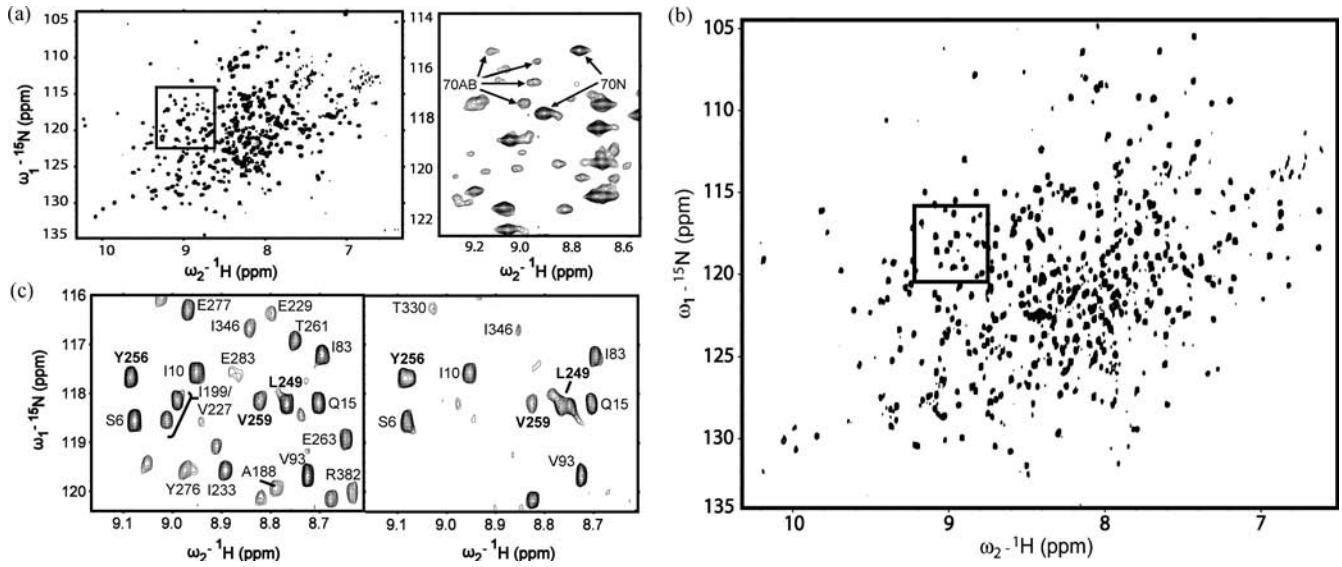

Figure 2. NMR analysis of RPA. (a) ^{15}N−^{1}H TROSY-HSQC of ^{15}N-RPA70NAB recorded at 800 MHz, 25 °C, and pH 6.0 (right) with expansion of the boxed region (left). (b) ^{15}N−^{1}H TROSY-HSQC of ^{2}H,^{15}N-RPA recorded at 800 MHz, 25 °C, and pH 7.5. (c) Expanded views of the spectrum in the absence (left) and presence (right) of dT_{30}. Signals from RPA70 and RPA32 (bold) are labeled.

which revealed three important observations. First, ssDNA has essentially no effect on RPA70N or RPA32C, showing directly that they play no role in the binding of ssDNA and remain available for functioning in the recruitment of other DNA processing factors. Second, the changes in signals of RPA70A and RPA70B upon binding of ssDNA were very similar to those observed when ssDNA is titrated into isolated RPA70AB. In addition, the signals from the A and B domains are seen to broaden upon binding of ssDNA, consistent with a tighter association of the tandem high affinity domains with the trimer core, which slows their rate of tumbling and increases the rate of relaxation. These results represent the first direct observation of the remodeling of RPA structural dynamics upon binding ssDNA and reflect DNA-induced alignment of RPA70AB with the trimer core.

The third important observation was that binding of ssDNA caused changes in the NMR signals of RPA32N, which also reflected remodeling of RPA. Comparison of NMR spectra for the intact protein and the isolated RPA32N domain revealed offsets in the intact protein until ssDNA is added (Figure S3). Since the 32N domain is the primary site for RPA phosphorylation, the transient interactions of RPA32N may explain why RPA actively involved in DNA processing (i.e., DNA-bound) can be efficiently phosphorylated by ambient cell-cycle machinery or DNA damage transducers. This hypothesis is consistent with previous reports that RPA associated with ssDNA is more accessible to kinase activity than the free protein.[6] The change in availability of RPA32N may also help explain how damage-dependent phosphorylation of RPA32N participates in redirecting processing of the DNA substrate from replication to repair.[7]

The analysis of full-length RPA shows NMR can serve as an effective tool for evaluating the structural dynamics of challenging multidomain proteins. While many obstacles remain to understanding the intricate choreography of DNA processing, we have demonstrated that NMR can contribute insight into the structural dynamics of the corresponding macromolecular machinery.

Acknowledgment. We gratefully acknowledge Markus Voehler, Alexey Bochkarev, Cheryl Arrowsmith, and Ellen Fanning, for valuable reagents and useful discussions, and support from the NIH (RO1 GM065484, T32 GM008320, PO1 CA092584, P30 CA068485, P50 ES000267).

Supporting Information Available: Experimental methods and supplementary Figures S1−S3. This material is available free of charge via the Internet at http://pubs.acs.org.

References

(1) Stauffer, M. E.; Chazin, W. J. *J. Biol. Chem.* **2004**, *279*, 30915–30918.
(2) (a) Iftode, C.; Daniely, Y.; Borowiec, J. A. *Crit. Rev. Biochem. Mol. Biol.* **1999**, *34*, 141–180. (b) Fanning, E.; Klimovich, V.; Nager, A. R. *Nucleic Acids Res.* **2006**, *34*, 4216–4137.
(3) Riek, R.; Fiaux, J.; Bertelsen, E. B.; Horwich, A. L.; Wüthrich, K. *J. Am. Chem. Soc.* **2002**, *124*, 12144–12153.
(4) (a) Tugarinov, V.; Kay, L. E. *J. Mol. Biol.* **2003**, *327*, 1121–1133. (b) Horst, R.; Bertelsen, E. B.; Fiaux, J.; Wider, G.; Horwich, A. L.; Wüthrich, K. *Proc. Natl. Acad. Sci. U.S.A.* **2005**, *102*, 12748–12753. (c) Helgstrand, M.; Mandava, C. S.; Mulder, F. A.; Liljas, A.; Sanyal, S.; Akke, M. *J. Mol. Biol.* **2007**, *365*, 468–479. (d) Hsu, S. T.; Fucini, P.; Cabrita, L. D.; Launay, H.; Dobson, C. M.; Christodoulou, J. *Proc. Natl. Acad. Sci. U.S.A.* **2007**, *104*, 16516–16521.
(5) Arunkumar, A. I.; Stauffer, M. E.; Bochkareva, E.; Bochkarev, A.; Chazin, W. J. *J. Biol. Chem.* **2003**, *278*, 41077–41082.
(6) (a) Fotedar, R.; Roberts, J. M. *EMBO J.* **1992**, *11*, 2177–2187. (b) Blackwell, L. J.; Borowiec, J. A.; Mastrangelo, I. A. *Mol. Cell. Biol.* **1996**, *16*, 4798–4807. (c) Fang, F.; Newport, J. W. *J. Cell Sci.* **1993**, *106*, 983–994.
(7) (a) Binz, S. K.; Sheehan, A. M.; Wold, M. S. *DNA Repair* **2004**, *3*, 1015–1024. (b) Zuo, Y.; Liu, Y.; Wu, X.; Shell, S. M. *J. Cell. Physiol.* **2006**, *208*, 267–273.

JA9013634